

Machine Learning-Based Uncertainty Quantification of Passive Intermodulation in Aluminum Contact

*Original*

Machine Learning-Based Uncertainty Quantification of Passive Intermodulation in Aluminum Contact / Treviso, Felipe; Trincherò, Riccardo; Canavero, Flavio G.. - ELETTRONICO. - (2022), pp. 1-4. ( 2022 3rd URSI Atlantic and Asia Pacific Radio Science Meeting (AT-AP-RASC) Gran Canaria, Spain 30 May 2022 - 04 June 2022) [10.23919/AT-AP-RASC54737.2022.9814426].

*Availability:*

This version is available at: 11583/2969970 since: 2022-07-08T19:25:49Z

*Publisher:*

IEEE

*Published*

DOI:10.23919/AT-AP-RASC54737.2022.9814426

*Terms of use:*

This article is made available under terms and conditions as specified in the corresponding bibliographic description in the repository

*Publisher copyright*

IEEE postprint/Author's Accepted Manuscript

©2022 IEEE. Personal use of this material is permitted. Permission from IEEE must be obtained for all other uses, in any current or future media, including reprinting/republishing this material for advertising or promotional purposes, creating new collecting works, for resale or lists, or reuse of any copyrighted component of this work in other works.

(Article begins on next page)

## Machine Learning-Based Uncertainty Quantification of Passive Intermodulation in Aluminum Contact

Felipe Treviso<sup>(1)</sup>, Riccardo Trincherò<sup>(1)</sup>, and Flavio G. Canavero<sup>(1)</sup>

(1) Department of Electronics and Telecommunications, Politecnico di Torino, Torino, Italy.

### Abstract

This paper deals with the development of a surrogate model for the uncertainty quantification and the stochastic analysis of passive intermodulation (PIM) in an Aluminum-Aluminum contact based on the least-squares support vector machine (LS-SVM) regression. Starting from a small set of training pairs collecting the configuration of the uncertain parameters and the corresponding PIM level, the LS-SVM allows to build a closed-form approximation of such non-linear relationship. Such model, can be suitably used within a Monte Carlo (MC) scenario in order to accelerate the simulation process and provide all the statistical quantities of interest. The results show a considerable speed-up on the computational time compared to a plain MC simulation, while achieving an accurate approximation of the PIM probability density function.

### 1 Introduction

Electronic systems may observe interference produced by passive intermodulation (PIM). This interference is characterized by spurious harmonic components produced by undesirable non-linearities arising in the passive elements of the system. Such spurious components can seriously threaten the quality of communication systems, as intermodulation products may fall into the receiving band or close to carrier frequencies, making their elimination through filters difficult [1, 2] and leading to electromagnetic interference (EMI) issues. One of the main sources of PIM in common electronic systems are the tunnel and thermionic emission effects in electric contacts, where thin oxide films might naturally be formed, deteriorating the conduction between the contact surfaces. Therefore, a good system design must take into account the evaluation of the PIM levels, as well as their possible impact of the system operating condition and reliability.

A few analytical models are available in the literature to estimate the PIM generated by non-ideal electric contact. The common idea is to replace the perfect contact by an equivalent non-linear circuit taking into account all the non-ideal effects (e.g., constriction resistance, film capacitance, etc.) [2, 3, 4, 5]. By considering as input the physical parameters of the contact, such model divides the nominal contact area  $A_n$  into 3 regions (see Fig. 1): (i) areas with a metal-

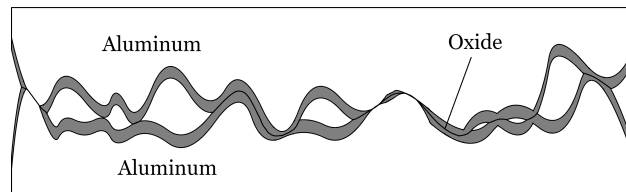


**Figure 1.** Illustrative figure of the interface between two metallic surfaces.

metal (MM) interface, where the oxide film at the surfaces was ruptured by the contact; (ii) areas with a metal-insulator-metal (MIM) interface, where the surfaces are in contact but the film is still present; (iii) areas in which the contact surfaces do not touch each other. Each region has its own effect on the electrical behavior of the contact, and it is embedded within the contact model in Fig. 2 (e.g., the non-linear effect of the MIM region is provided by the non-linear resistance  $G_f$ ).

Nonetheless, it is hard to know in a deterministic way the exact values for all the input parameters of such models. As an example, the ones related to the contact surface are intrinsically statistical in nature (e.g., the average radius of surface asperities). On the other hand, some of them are extremely uncertain, since they strongly depend on the uncontrollable randomness introduced by the manufacturing process. In this regard, the PIM levels predicted by such analytical models will always come with some degree of uncertainty, and thus requiring a statistical assessment. In the above scenario simulations turn out to be the most efficient and cheap approach to carry out a statistical assessment during the design phase, compared to the most expensive and time consuming one based on the experimental measurements and prototypes [6, 7]. However, it is well known that a plain Monte Carlo analysis turns out to be extremely inefficient when the model is slow to be evaluated. This paper proposes to apply a machine learning regression technique, namely, the least-squares support vector machine (LS-SVM) regression [7, 8], to construct a closed-form and fast to evaluate surrogate model in order to accelerate the stochastic evaluation of the production of PIM in an aluminum-aluminum contact. Specifically, a parametric circuitual model for the contact is estimated through the analytical models available in the literature [2, 3, 4, 5]. Such model is then simulated for a small set of configurations of

the input parameters drawn according to their probability distribution and provides as output the corresponding level for the 3rd order PIM product. The configurations of the input parameters are used together with the PIM level to train a surrogate model based on the LS-SVM regression. Such model can be used to inexpensively generate the large number of PIM predictions needed to perform the advocate statistical analysis (e.g., to obtain the probability distribution of the output in a fast and efficient way).

## 2 PIM Simulation

The circuitual model used for PIM prediction is shown in Fig. 2. In the Figure, the highlighted block is the *contact model* which takes into account the effects of a realistic contact degraded by a thin oxide film and in which the values of the elements depend on the physical parameters of the contact [2, 3, 4, 5], whereas  $V_s$  and  $R_s$  represent the Thevenin equivalent of the rest of the system. The element  $G_f(V_{Gf})$  is a non-linear conductance written as a polynomial function, which depends on the voltage  $V_{Gf}$ , providing the source of non-linearity in the circuit. The circuit is analyzed in time-domain via a transient simulation in HSPICE and the PIM products are extracted from the corresponding spectrum computed by means of the Fast Fourier transform (FFT). In this work,  $R_s = 2 \Omega$ ,  $V_s$  is a 900 MHz sinusoidal signal with 0.45 V amplitude, and the FFT is applied to 21 periods of steady-state simulation to convert the results to the frequency-domain. The third intermodulation product, given in dBm, is computed as

$$PIM = 10 \log(\Re \{V_{3f_0} I_{3f_0}^* / 2\}) + 30, \quad (1)$$

where  $V_{3f_0}$  and  $I_{3f_0}$  are, respectively, the contact voltage and current amplitude at 2.7 GHz.

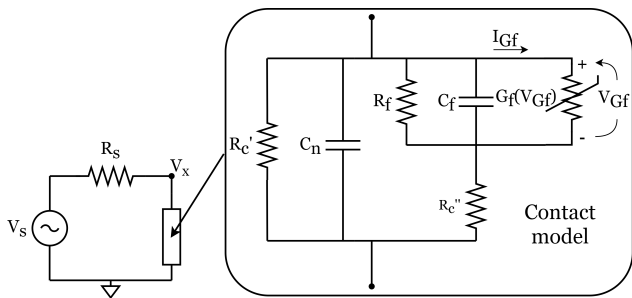


Figure 2. Equivalent circuit.

Table 1 lists, along with a short description, all the parameters used as input to compute the values of the components in the circuit equivalent in Fig. 2. The list consists of 18 parameters, among which we can cite the contact surface rugosity, the mechanical and electrical properties of the material, and the contact design and operation characteristics., (e.g., its nominal area, temperature and contact force). It is important to remark that all the parameters collected in Table 1 are considered uncertain and thus are modeled as a set of 18 uncorrelated and uniform distributed random

variables defined by a nominal value and their corresponding variation around such value. The above uncertainty on the parameter values may come either from natural fluctuations during the contact operation, like in the case of the temperature, or from lack of detailed information on their characterization, e.g., the standard deviation of the rugosity profile and density of asperities in the surface that are characterized from a few measured samples. Three different values for such variation are considered: for parameters better known and controlled, only a 2 % variation is used, while for other parameters that are less controllable, a 5 or even 10 % variation is considered. The parameter  $\mu$  has zero mean and thus cannot have its variability expressed by a relative value. Therefore, it is set as  $\pm 30$  nm.

Table 1. Input parameters for the model of an aluminum electric contact.

Par.	Nominal val.	Var.	Description
$\eta$	$3 \times 10^4 \text{ mm}^{-2}$	10%	Density of asperities
$\sigma$	$2.0 \mu\text{m}$	10%	Std. of rugosity profile
$\mu$	0	30 nm	Mean value of rugosity
$R_a$	$30 \mu\text{m}$	10%	Surface asperities radius
$F$	0.1 N	10%	Contact force
$A_n$	$1 \text{ cm}^2$	5%	Nominal area
$T$	$30 \text{ }^\circ\text{C}$	10%	Contact temperature
$\rho_f$	$1 \times 10^9 \Omega\text{m}$	2%	Resistivity of the film
$s$	$15 \text{ \AA}$	10%	Average film thickness
$\epsilon_f$	9	2%	Dielectric constant of film
$\phi_f$	4.97 eV	2%	Work function of film
$\alpha$	0.4	10%	Cracking effect par.
$E_g$	2.5 eV	2%	Band gap of film
$\rho_1$	$27 \text{ m}\Omega \mu\text{m}$	2%	Al. resistivity
$\phi_1$	4.08 eV	2%	Al. work function
$E_1$	70 GPa	5%	Al. Young modulus
$\nu_1$	0.33	5%	Al. Poisson ratio
$\lambda_0$	0.46	5%	Richardson constant coef.

In order to reduce the numerical noise to values lower than the PIM when converting the data from time to frequency domain, the circuitual simulation of this analytical model should be performed with maximum accuracy and for many time steps. In the simple system analyzed in this paper, each simulation takes 1.9 s to be completed. An uncertainty quantification requires several thousands evaluations, with possibly more complex systems, making it a slow task. In order to speed up the analysis, a LS-SVM surrogate model is used. After the surrogate model is trained, it allows a closed-form evaluation of the PIM, without requiring the long numerical simulation used with the circuitual model.

## 3 Least-Square Support Vector Machine Regression

The LS-SVM regression is a learning method for classification or regression characterized by the use of a kernel and of Tikhonov regularization to prevent over-fitting [8]. The LS-SVM regression searches to approximate a set of train-

ing data pairs  $\{(\mathbf{x}_k, y_k)\}$  for  $k = 1 \dots L$ , with a non-linear regression  $\tilde{y} = \mathcal{M}(\mathbf{x})$ , with the input  $\mathbf{x} = [x_1, \dots, x_d]^T \in \mathbb{R}^d$  and output  $y \in \mathbb{R}$ . The dual space formulation of the LS-SVM regression model is the following [8]:

$$\tilde{y}(\mathbf{x}) = \sum_{k=1}^L \alpha_k k(\mathbf{x}_k, \mathbf{x}) + b, \quad (2)$$

where  $\alpha = [\alpha_1, \dots, \alpha_L]^T$  are the coefficients of this dual space model,  $b \in \mathbb{R}$  is a constant term and  $k(\mathbf{x}_k, \mathbf{x})$  is the so called kernel function, which provides an implicit mapping between the parameter space and a non-linear feature space. The most adopted kernel function is the radial basis function (RBF) kernel, tuned by its hyperparameter  $\sigma$  and given by

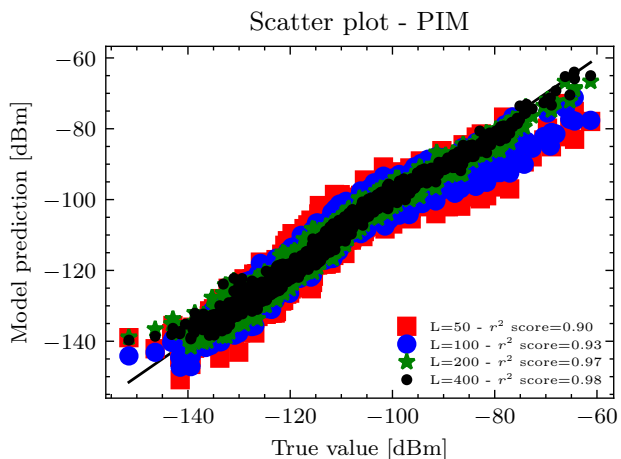
$$k(\mathbf{x}_k, \mathbf{x}) = \exp(-|\mathbf{x} - \mathbf{x}_k|^2 / (2\sigma^2)). \quad (3)$$

The unknowns  $\alpha$  and  $b$  are computed by solving the following linear system of equations [8]:

$$\begin{bmatrix} \Omega + \mathbf{I}^L / \gamma & \mathbf{1} \\ \mathbf{1}^T & 0 \end{bmatrix} \begin{bmatrix} \alpha \\ b \end{bmatrix} = \begin{bmatrix} \mathbf{y} \\ 0 \end{bmatrix}, \quad (4)$$

where  $\gamma$  is the regularization hyperparameter and  $\Omega_{i,j}$ , the element on the  $i$ -th row and  $j$ -th column of the  $L \times L$  kernel matrix  $\Omega$ , computed as  $\Omega_{i,j} = k(\mathbf{x}_i, \mathbf{x}_j)$ .

A LS-SVM model for the  $PIM$  in (1) is trained over a limited quantity of samples  $L$  from the circuital model by solving (4) and optimizing the hyperparameters  $\gamma$  and  $\sigma$  via a 5-fold cross-validation procedure. This quantity  $L$  is much smaller than the number of samples required to perform the uncertainty quantification, which can then be performed over the much faster surrogate model, with little loss of accuracy.



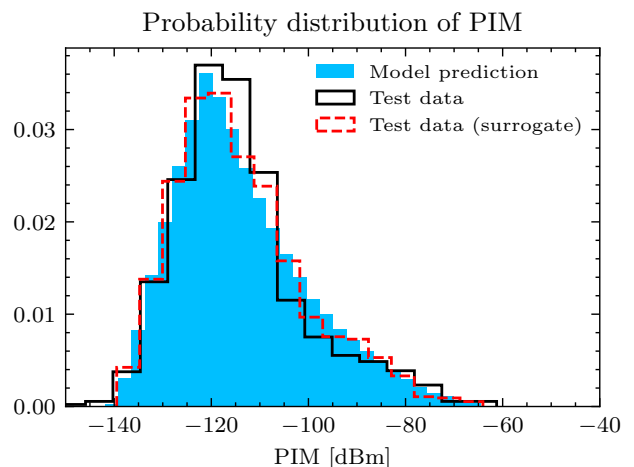
**Figure 3.** Scatter plot comparing the output of the LSSVM model for  $PIM$  to the true value.

Figure 3 shows a scatter plot over 1600 test samples comparing the output of the LSSVM model for  $PIM$  to the true value of the circuital simulation, for different numbers of training samples. It is possible to observe that starting with 50 training samples, the surrogate model already follows

considerably the pattern of the true model, albeit with some inaccuracies. The increase in the number of samples provides better models, and at  $L = 400$  training samples the model is already very accurate, giving a  $r^2$ -score of 0.98.

## 4 Uncertainty Quantification

The output variability of  $PIM$  can be analyzed by performing a Monte Carlo (MC) simulation using the stochastic description of the input parameters from Table 1. The surrogate model is evaluated on 100,000 samples. The resulting probability density function for the  $PIM$  level obtained for the above analysis is shown given in the blue histogram in Fig. 4. As a comparison, histograms with 1600 samples from the true model and the surrogate are also plotted, respectively, in black and red, to validate this stochastic analysis. Both histograms are similar to each other, albeit the reduced number of samples make them less smooth than the probability distribution obtained in blue. Overall, the output probability distribution gives a mean value for the  $PIM$  equal to -113.8 dBm, and a standard deviation of 13.7 dBm.



**Figure 4.** Histogram for the  $PIM$  obtained by the MC simulation via the surrogate model compared to the test data.

The  $PIM$  histogram presents a wide span in its value, going from -142 dBm to -56 dBm, even though the inputs had less than 10% variation. This highlights the fact that the  $PIM$  is a highly non-linear phenomenon, in which small changes in the contact design can lead to issues. Nonetheless, if the system being analyzed requires a maximum  $PIM$  level of -97 dBm [1] in order to function reliably, this MC analysis has shown that there is a 12.9% probability that the studied contact produces a  $PIM$  higher than that threshold. It is a rather risky probability, and thus this design should receive more work on the reduction of  $PIM$  or in its robustness to intermodulation interference, and this can be done before building expensive prototypes due to the performed analysis. This probability is similar to what is observed in the 1600 test samples, where 11.1% of samples were larger than the threshold, when we analyze the circuital model, and 12.3% in the surrogate model, additionally validating the surrogate model. This comparison is shown in Fig. 5.

Regarding the computational time, the speed-up provided by the LS-SVM surrogate is its main advantage. While the full circuital model in Fig. 2 requires 1.9 s per simulation, the LS-SVM model trained with 400 samples can evaluate the output 100,000 times in only 37.7 s, a rather negligible time per sample. Its main computational cost comes from its training, which takes 28.6 s, and from the simulation of 400 training samples on the true circuital model, which takes around 760 s. In total, 826.3 s are required for the uncertainty quantification via the surrogate model. A similar approach using the original model would take 52.8 h (190,000 s). Based on these numbers, the LS-SVM-based surrogate model is able of providing a speed-up of 250 times compared to a classical MC simulation.

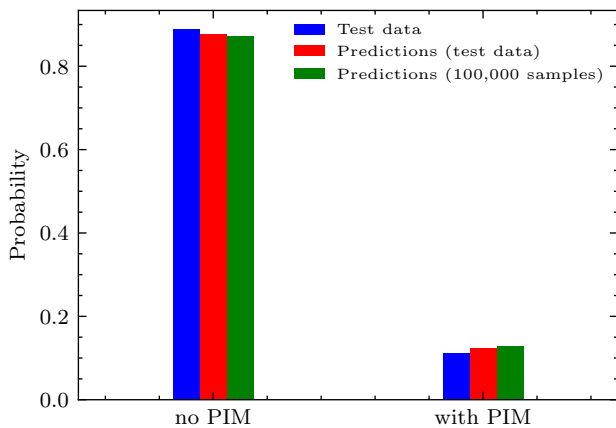


**Figure 5.** Diagram with the probability that the output presents a PIM value larger or smaller than the defined threshold.

## 5 Conclusions

The statistical evaluation of PIM produced by an electrical contact is essential to avoid EMI issues. Such evaluation, however, can only realistically be performed via theoretical models analyzed via circuital simulators. Those circuital simulations are still time consuming, but the use of accurate LS-SVM surrogate model is able to speed-up considerably the required statistical analysis. The resulting workflow provides a quick way to analyze a certain contact design and statistically evaluate the PIM level that can be introduced to the system by the contact. The performed analysis provides to the designer the expected PIM so that he can rearrange the design accordingly without the need of building possibly expensive prototypes, while also avoiding subsequent surprises.

## 6 Acknowledgements

This material is based upon work supported by Huawei Technologies Oy (Finland) Co. Ltd. under contract YBN2020055131. The Authors would like to thank Petri Keski-Opas and Ilkka Kelander for the valuable and constructive discussions during the development of this work.

## References

- [1] Anritsu Company (2014). Understanding PIM (Application Note 11410-00629F). Retrieved on 2/Dec/2021 from: <https://dl.cdn-anritsu.com/en-us/test-measurement/files/Application-Notes/Application-Note/11410-00629F.pdf>
- [2] Q. Jin, J. Gao, G. T. Flowers, Y. Wu and G. Xie, "Modeling of Passive Intermodulation With Electrical Contacts in Coaxial Connectors," in *IEEE Transactions on Microwave Theory and Techniques*, vol. 66, no. 9, pp. 4007-4016, Sept. 2018.
- [3] S. Zhang, X. Zhao, Z. Cao, K. Zhang, F. Gao and Y. He, "Experimental Study of Electrical Contact Non-linearity and its Passive Intermodulation Effect," in *IEEE Transactions on Components, Packaging and Manufacturing Technology*, vol. 10, no. 3, pp. 424-434, March 2020.
- [4] C. Vicente and H. L. Hartnagel, "Passive-intermodulation analysis between rough rectangular waveguide flanges," in *IEEE Transactions on Microwave Theory and Techniques*, vol. 53, no. 8, pp. 2515-2525, Aug. 2005.
- [5] F. Treviso et al. "Sensitivity Analysis of Passive Intermodulation due to Electrical Contacts," in *IEEE Transactions on Electromagnetic Compatibility*, accepted for publication. DOI (identifier) 10.1109/TEM.C.2022.3142963
- [6] P. Manfredi, D. Vande Ginste, D. De Zutter and F. G. Canavero, "Uncertainty Assessment of Lossy and Dispersive Lines in SPICE-Type Environments," in *IEEE Transactions on Components, Packaging and Manufacturing Technology*, vol. 3, no. 7, pp. 1252-1258, July 2013.
- [7] R. Trincherro, P. Manfredi, I. S. Stievano and F. G. Canavero, "Machine Learning for the Performance Assessment of High-Speed Links," in *IEEE Transactions on Electromagnetic Compatibility*, vol. 60, no. 6, pp. 1627-1634, Dec. 2018, doi: 10.1109/TEM.C.2018.2797481.
- [8] J.A.K. Suykens *et al.*, "Least Squares Support Vector Machines", World Scientific, Singapore, 2002 (ISBN 981-238-151-1).